JCTC Journal of Chemical Theory and Computation

Quantum Mechanical Quantification of Weakly Interacting Complexes of Peptides with Single-Walled Carbon Nanotubes

Wenjie Fan,[†] Jun Zeng,[‡,§] and Ruiqin Zhang*,[†]

Centre of Super-Diamond and Advanced Films (COSDAF) and Department of Physics and Materials Science, City University of Hong Kong, Hong Kong SAR, China, MedChemSoft Solutions, P.O. Box 5143, Wantirna South, VIC 3152, Australia, and College of Chemistry, Sichuan University, Chengdu 610064, China

Received May 18, 2009

Abstract: We investigated the binding nature of three peptides (inactive NB1 and active B1 and B3) to single-walled carbon nanotubes (SWCNTs) using a density functional tight-binding (DFTB) method with an empirical van der Waals force correction. We show that the three peptides could be spontaneously adsorbed to the carbon nanotube (CNT) surface through $\pi-\pi$ and/or H$-\pi$ stacking at physisorption distances and the geometric and π-electronic structures of SWCNTs remain basically undamaged upon the adsorption. We also investigated the diameter and chirality dependence of binding energies. The calculated results are consistent with experimental observation, and we found that aromatic residues, such as His and Trp, are the keys in determining peptide/CNT binding. In addition, our calculations predict that noncovalent modification of SWCNTs by the active peptides might increase the electron transfer capabilities of SWCNTs.

1. Introduction

Carbon nanotubes (CNTs), discovered in 1991 by Iijima,[1] have many novel electrical and mechanical properties, such as high electrical conductivity, excellent stiffness against bending, and high tensile strength.[2] Single-walled carbon nanotubes (SWCNTs) have potential biological applications ranging from biomedical sensors to drug delivery.[3−5] But such biological applications have, so far, been limited owing to two major obstacles: hydrophobicity and conformational heterogeneity. Although the solubility in water can be improved by chemically modifying the SWCNTs through covalent bonding of various functional groups to the nanotubes,[6,7] these modifications can perturb the intrinsic properties of SWCNTs, such as electrical properties. As a result, alternative approaches using the noncovalent adsorption of surfactants,[8] polymers,[9] and biomolecules[10−12] to solubilize the SWCNTs have been proposed and tested.

In recent years, much research attention has focused on the design and utilization of polypeptide/CNT complexes because of their functionality in biological systems.[13−18] Encircling CNTs with peptides has two major advantages:[15] (1) the peptides will not dissociate from the CNTs thereby providing extremely stable CNT dispersions and (2) this method enables the diameter selective separation of SWCNTs,[15] since nanotubes with a specific diameter are preferentially circled by a given length of peptides. For example, to improve CNT solubility in water as well as biocompatibility, Zorbas et al. developed a family of amphiphilic helical peptides that noncovalently bind and solubilize SWCNTs in water, yielding unbundled and individual SWCNTs.[14] Later they devised a novel way to coat SWCNTs with reversible cyclic peptides to separate them based on differences in diameters.[15]

Despite these exciting experimental observations, many outstanding questions remain regarding the affinity of selected peptide/SWCNTs complexes. For example, how

* Corresponding author. E-mail: aprqz@cityu.edu.hk.
[†] City University of Hong Kong.
[‡] MedChemSoft Solutions.
[§] Sichuan University.

10.1021/ct9002493 CCC: $40.75
Published on Web 09/11/2009

does the type of carbon-based nanomaterial differ in the selection for peptide sequence? Do peptide sequences selected for one kind of carbon-related nanomaterials preserve the high attraction for other forms? As an initial step in exploring these critical questions, we investigated the binding feature between SWCNTs and three representative peptides, namely, inactive peptide NB1 and active peptides B1 and B3. The present research is a theoretical contribution to the binding features of biomolecule/nanomaterial complexes in the gas phase.

2. Computational Details

Weak interactions exist widely and play a significant role in determining and stabilizing the three-dimensional structures of proteins. In proteins, the weak interactions among aromatic side chains, backbone amides, carboxyl groups, aliphatic hydrogen atoms, and other parts exist widely. Individually, these interactions might be weak but when combined they have a large influence on the conformational stability of a protein.[19,20] For example, the arene−arene and arene−COO interactions were reported to complicate the measurement of the UV absorption of residues.[21]

The peptides adsorbed on the surface of SWCNTs might be a proto-typical weakly interacting complex that involves π bonding; this remains a challenging issue for theoretical studies because these systems cannot be described correctly by conventional DFT or methods based on classical interatomic potentials. MP2 and CCSD theories are used as standard methods to consider the dispersion force,[22,23] but for large systems of biological interest, such methods are not applicable. In this study, we used a computationally efficient approximation to density functional theory, the self-consistent charge density functional tight-binding (SCC-DFTB) scheme, complemented by the empirical London dispersion energy term (acronym DFTB-D) to study the energy and geometry structure of the three peptides in relation to the CNTs. The SCC-DFTB model has been derived from a second-order expansion of the DFT total energy functional with respect to charge density fluctuations; at the same time, the Hamiltonian matrix elements are calculated with a two-center approximation. These are then tabulated together with the overlap matrix elements with respect to interatomic distance. A comprehensive description of the method can be found in the literature.[24,25] The van der Waals interaction has been described with an empirical dispersion term, consisting of an R^{-6}, term added to the SCC-DFTB total energy.[26,27] The SCC-DFTB-D has been successfully applied to investigating the energies and structures of biomolecules.

In this work, we considered SWCNTs with different chiralities, saturated at the ends by hydrogen atoms. The CNTs we studied are armchair (n, n) $(n = 3-6)$, zigzag (8,0) tube, and chiral (6,3) tube. The tube length is around 33 Å, which is long enough to eliminate the effect of the terminal hydrogen atoms. We investigated three representative peptides, including the peptide NB1 of sequence LPPSNASVADYS, the peptide B1 of sequence HWKHPWGAWDTL, and the peptide B3 of sequence HWSAWWIRSNQS. Peptides NB1 and B1 were initially constructed as fully extended structures. For B3, previous CD experiments have demonstrated that the free B3 peptide adopts a helical conformation at a neutral pH value and the binding to SWCNTs does not affect its helical conformation.[18] Therefore, in this work, we considered the initial structure of peptide B3 as a helical conformation. We first positioned the arene clusters in these peptides approximately parallel to the sidewall of the SWCNTs, with part of them making direct contact, followed by full geometric optimizations using conjugate gradient algorithm until the residual forces were below 2×10^{-4} au; we set the charge convergence criterion to be 10^{-5} electrons.

To provide a better understanding of the electronic properties of the peptide/CNT complexes, we investigated the density of states (DOS) of the active complexes. The DOS was calculated using the SIESTA method.[28,29] We used the Ceperley−Alder version of the LDA[30] for the electron exchange and correlation as well as optimized Troullier−Martins pseudopotentials[31] for the atomic cores in this calculation. We performed the computations of this part using a supercell approach and periodic-boundary conditions. We adopted a lateral separation of 35 Å between the tube centers, which was large enough to eliminate the interaction between the neighboring tubes. We then used two Monkhorst−Pack k points for the Brillouin zone integration along the tube axis. A cutoff of 150 Ry for the grid integration was utilized, representing the charge density. Although different models might result in different optimized structures and, thus, different electronic properties, this effect can be eliminated if the tube length is long enough to eliminate the interaction between the peptide and the hydrogen atoms at the tube ends and the lateral separation between tube centers is large enough to eliminate the interaction between the neighboring tubes. In our work, the binding energies for the cluster and the periodic models were respectively almost the same, as were the optimized structures for the interacting parts for both models.

3. Results and Discussion

3.1. Structures and Binding of the Peptide/CNT Complexes. Figures 1a−c show the optimized structures for the three peptides. NB1 involves only one arene (Tyr) at the 11th position. B1 in which an extended conformation is adopted involves five arenes: three tryptophans at the second, sixth, and ninth positions and two histidines at the first and fourth positions, respectively. For the helical peptide B3, the structure is relatively compact as a result of the intramolecular hydrogen bonds. One representative intramolecular hydrogen bond is formed between C═O of the Trp2 and N−H of the Trp6 positions with N−O and H−O distances of 2.91 and 1.90 Å, respectively.

Figure 2 shows the optimized geometries of the three peptides/(5,5) CNT complexes. We calculated the binding energies of the studied systems with the following equation: $E_B = E_{(\text{peptide/SWCNT})} - E_{(\text{SWCNT})} - E_{(\text{peptide})}$, where $E_{(\text{SWCNT})}$ and $E_{(\text{peptide})}$ are the total energy of the isolated pristine tube and peptide, respectively, and $E_{(\text{peptide/SWCNT})}$ is the total energy of the peptide/SWCNT complex.

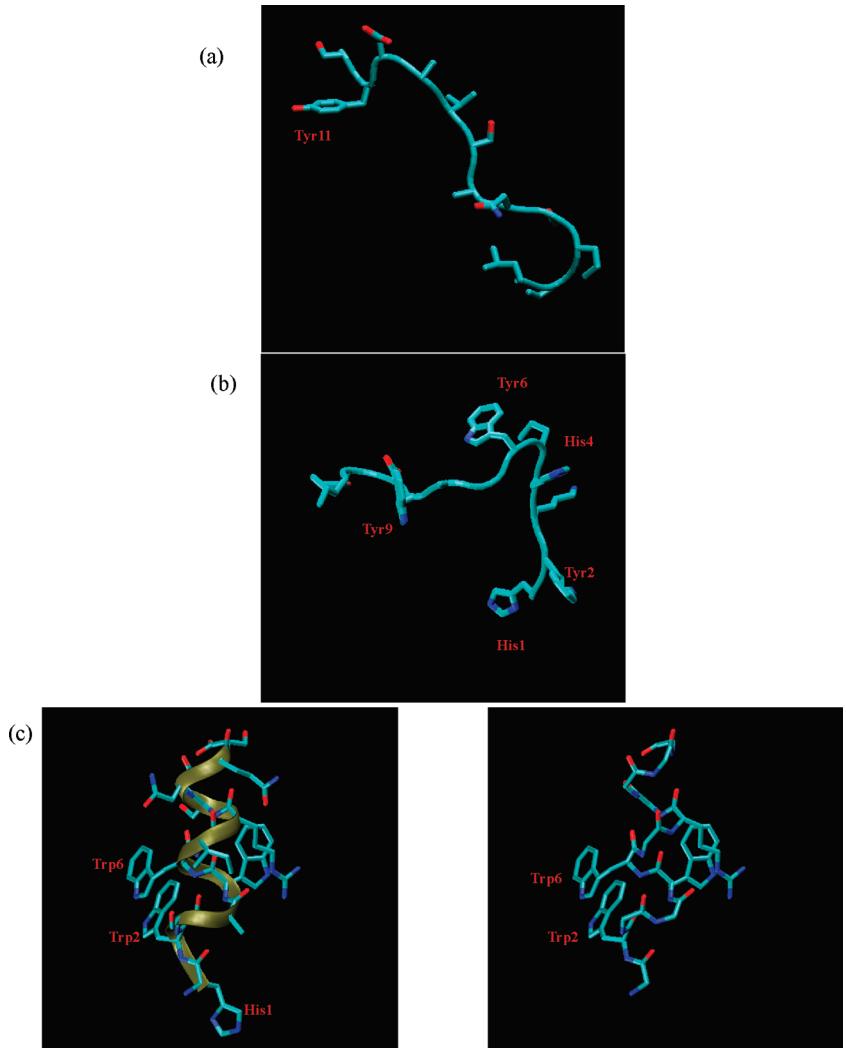

Figure 1. Optimized structures for (a) peptide NB1, (b) peptide B1, and (c) peptide B3. The important aromatic residues are labeled in red.

Upon adsorption to the CNTs, the three peptides show different binding features. For the inactive peptide NB1 (shown in Figure 2a), the contact area of peptide NB1 with the (5,5) CNT surface is located at the aromatic ring of Tyr11. The phenol ring is adsorbed to the CNT surface in a parallel manner by a favorite "bridge site" with a nearest C−C distance of 3.00 Å. The binding energy is calculated to be −0.71 eV. Since little contact occurs between the CNT and the other parts in NB1, the geometry of peptide NB1 undergoes little change upon adsorption.

The active peptide B1 wraps around the (5,5) CNT surface, as shown in Figure 2b. Compared with isolated B1 in Figure 1b, most of the peptide interacts with the CNT surface, and the adsorbed B1 shows obvious conformational changes to facilitate maximum interaction with the surface. First, the aromatic ring of the N-terminal residue His1 is turned parallel to the tube surface, with the nearest distance between the C−C around 3.14 Å. Second, of all three Trp residues, Trp2 and Trp6 adopt a favorable parallel orientation to the CNT surfaces. However, Trp9 is tilted to the CNT surface due to the sterical effect. For the Trp2 ring that is favorably bonded to the CNT surface by $\pi-\pi$ stacking, the nearest distance between the C−C is around 3.02 Å. While the His1 is close to the tube surface, the His4 is perpendicular to the tube. Since the CNT is circled by the peptide B1, the contact area is much larger than that of NB1/CNT. Third, several XH$-\pi$ (X = C or N) interactions occur between the peptide B1 and the CNT surface. While a NH$-\pi$ interaction is found between the backbone amide of Trp2 and the CNT surface with a N−C distance of 3.25 Å and a H−C distance of 2.28 Å, respectively, a weaker CH$-\pi$ interaction is identified between the Cα of Lys3 and the CNT surface, with a shortest C−C distance of 3.48 Å and a H−C distance of 2.47 Å, respectively. The overall binding energy is calculated to be −2.85 eV.

For active peptide B3 with a helical conformation, the binding energy to the (5,5) CNT is predicted to be −2.22 eV. Figure 2c shows the adsorbed peptide on the CNT surface. Compared with the isolated peptide, the adsorption has minor effect on the peptide's helical conformation. Similar to active peptide B1, peptide B3 binds to the CNT surface via the favorable $\pi-\pi$ stacking between the CNT surface and the aromatic residues His1, Trp2, and Trp5, with the corresponding N−C and C−C distances calculated to be 3.21 and 3.05 Å, 3.34 and 2.94 Å, and 3.22 and 3.06 Å, respectively. Moreover, the $\pi-\pi$ stacking clusters Trp2/Trp6

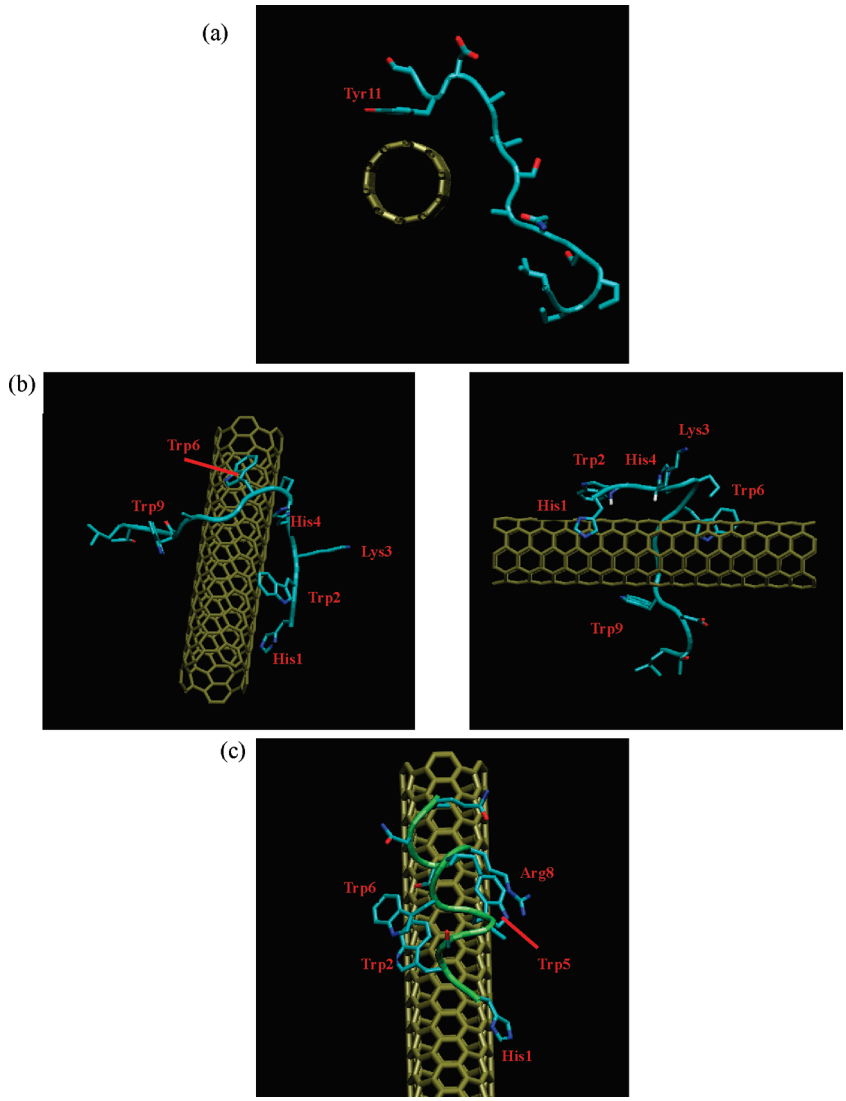

Figure 2. Illustration of the peptide/(5,5) CNT interactions: (a) inactive peptide NB1, (b) the active peptide B1, and (c) the active peptide B3. The $\pi-\pi$ stacking and XH$-\pi$ (X = C and N) interactions are displayed in the left and right panels for the (b) B1/CNT complex, respectively. Key residues are labeled in red.

and Trp5/Arg8 found in the isolated peptide (Figure 1c) are well preserved in the B3/CNT complex, indicating that the $\pi-\pi$ interactions contribute not only to the binding activities of the peptide but also to the stabilization of the helical conformation. The preservation of the helical conformation upon peptide B3 adsorption to the side wall of SWCNT is consistent with the experimental observation obtained using CD spectroscopy.[18] Our results demonstrate that the geometric structure of CNT remains almost unchanged after the adsorption of peptides.

3.2. Diameter and Chirality Dependence of the Binding Energy for the Peptide/CNT Complexes. Figure 3 shows the diameter dependence of the binding energies of active peptide B1 to the (n, n) CNTs (n = 3−6) at a given tube length. Overall, the binding energies increase as the tube diameter grows larger, except at the beginning when n = 3 and 4; the peptide/(4,4) CNT binding is slightly higher than the binding of the peptide/(3,3) CNT. For the active B1 that encloses the CNTs, the contact area between the B1 and the CNT is large. When B1 is adsorbed to the CNT, the aromatic parts (such as His and Trp) in direct contact with the CNT

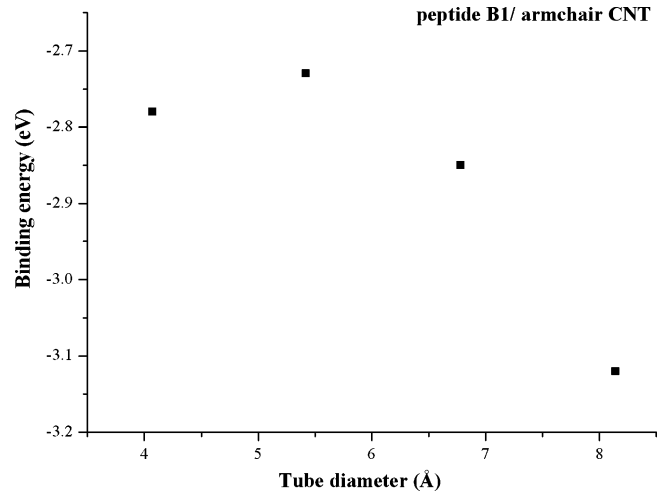

Figure 3. Diameter dependence of binding energies of B1 to the (n,n) CNT (n = 3−6) at a given tube length.

will undergo considerable conformation change to facilitate maximum intermolecular interactions with the CNT. This

Table 1. The Chirality Dependence of the Binding Energy for Peptide/CNT Complexes

	tube diameter (Å)	binding energies (eV)
NB1/(5,5) CNT	6.78	−0.71
NB1/(8,0) CNT	6.26	−0.67
NB1/(6,3) CNT	6.23	−0.64
B1/(5,5) CNT	6.78	−2.85
B1/(8,0) CNT	6.26	−2.82
B1/(6,3) CNT	6.23	−2.69
B3/(5,5) CNT	6.78	−2.22
B3/(8,0) CNT	6.26	−2.21
B3/(6,3) CNT	6.23	−1.97

will result in a change of B1 geometry arising from intramolecular interactions. In addition, the geometric change in peptide B1 will affect the intermolecular interactions between the CNT surface and peptide B1. This chain interaction will finally change the basic structure of the free peptide B1. As mentioned above, the interactions between B1 and CNT involve $\pi-\pi$, CH$-\pi$, and NH$-\pi$ interactions, and the competition of these weak interactions will determine the final equilibrium structures and binding energy. Therefore, we cannot simply assume that as the contact area increases, the binding energies will increase correspondingly, just as we found in 1-pyrenebutanoic acid, succinimidyl ester (PSE)/CNT.[32] We did not observe any linear relationship between the binding energy and the tube diameter for any of the three peptide/CNT complexes considered here.

We also studied the chirality dependence of the binding energy for peptides/CNT and considered three tubes with similar diameters: (5,5), (8,0), and (6,3) tubes. Table 1 gives the results. We found that, although the chirality dependence of the binding energies is not obvious, generally as the tube diameter increases, the binding energy will also increase. Of the three tubes considered here, the armchair (5,5) tube, with the largest tube diameter, has the largest binding energy, while the chiral (6,3) tube, with the shortest diameter, demonstrates the smallest binding energy.

3.3. Molecular Orbitals of the Peptide/CNT Complexes. Figure 4 presents the isosurfaces of the selected frontier orbitals for peptide B3/(5,5) CNT, pristine (5,5) CNT, and single B3 at a 0.01 au isovalue. For isolated B3, the highest occupied molecular orbital (HOMO) and the lowest unoccupied molecular orbital (LUMO) locate on the Arg and Trp2, respectively. After adsorption to the (5,5) CNT system, both the HOMO and LUMO locate on the (5,5) tube, and no molecular orbital overlapping occurs between the B3 and the (5,5) CNT. We conclude that the noncovalent $\pi-\pi$ stacking of B3 to CNTs does not damage the π-conjugation electronic structures of the CNTs. Our calculations show that after adsorption of B3 on the sidewall, the HOMO−LUMO gap for the CNT remains almost unchanged. These results suggest that the π-electronic properties of the CNT are preserved after noncovalent adsorption of B3, which is similar to the features for simple planar organic molecules adsorbed on CNTs.[33,34] We find similar orbital features for the NB1/(5,5) CNT and the B1/(5,5) CNT.

3.4. Electronic Properties. We sought further understanding of the electronic properties of peptide/CNT interactions by calculating the DOS of the peptide/CNT complexes.

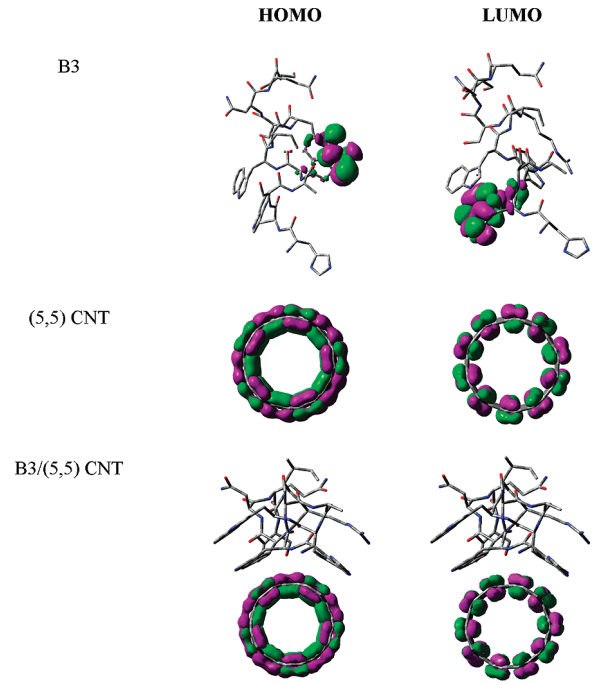

Figure 4. Isosurfaces of the selected frontier orbitals of the B3/(5,5) CNT complex at the ground state. The isovalue is 0.01 au.

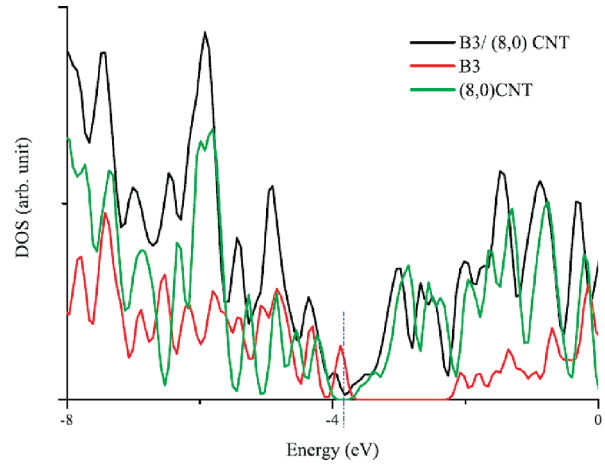

Figure 5. Total density of states for B3/(8,0) CNT.

We considered the metallic (5,5) CNT and the semiconducting (8,0) CNT to study the features of the DOS. Figure 5 shows the total DOS of the B3/(8,0) CNT. For the B3/metallic (5,5) CNT (not shown here), we find that the total DOS of the system preserves the DOS features of pristine (5,5) tube, and there isn't obvious new DOS induced near the Fermi level. But we find different binding features when B3 interacts with semiconducting (8,0) CNT. Compared with the pristine (8,0) CNT, the DOS of the B3/(8,0) CNT shows new states near the Fermi level, which were contributed by the peptide B3. Still, the nature of physisorption is shown since the total DOS preserves the features of the DOS of pristine (8,0) CNT. The Fermi energy level (E_f) of the semiconducting (8,0) CNT was predicted to be −3.86 eV, while for the B3/(8,0) CNT, the E_f was almost unchanged. We find new DOS, composed mainly of the HOMO of B3 molecular orbitals, between the (8,0) CNT conduction and

valence bands. Hence, the band gap of the system has sharply decreased from the pristine (8,0) tube 0.58 to 0.29 eV of the complexes. Similar finding of band gap reduction has been found in the (7,3) polyC−DNA complex compared to the free semiconducing (7,3) tube.[35] For the semiconducting (8,0) CNT, the band gap remains almost unchanged. For peptide B3, our calculations show that the band gap is enlarged slightly after adsorption. The finding of the new DOS formed between the (8,0) CNT conduction and valence bands is quite similar to our previous study of flavin adenine dinucleotide (FAD)/(10,0) CNT.[36] For the DOS of B1/(8,0) CNT (not shown here), we find similar features of the weak interaction: new states, composed mainly of the HOMO of the B1 molecular orbital, between the (8,0) CNT conduction and valence bands. Compared to pristine SWCNTs, the new states formed in the active peptides/(8,0) system may cause obvious increasing electron transfer abilities. A CV experiment is highly desirable to verify this observation.

We furthermore examined the charge transfer between the peptide B3 and the (8,0) CNT from an analysis of the Mulliken charges for the SCC-DFTB-D calculations. There is very small charge transfer (0.02e) observed from peptide B3 to (8, 0) tube. Again, the negligible charge transfer in this $\pi-\pi$ bonded system demonstrates the weak interaction nature of the peptide and CNT complexes.

Based on the above analysis of the structures and properties of the peptide/CNT complexes, we show that the arene parts, such as His and Trp, play a significant role in the noncovalent binding of peptides to the CNT surface. Our theoretical results confirm the experimental finding[37] and also agree with previous theoretical reports.[38,39]

4. Conclusions

We show via quantum mechanical investigation that peptides (inactive NB1 and active B1 and B3) could be spontaneously attracted to the sidewall of CNTs through $\pi-\pi$ and/or H$-\pi$ stacking, which is at the physisorption distance. The competition of $\pi-\pi$ and/or H$-\pi$ stacking plays a key role in binding the peptides to the CNTs, thus, determining and stabilizing the binding of the peptide/CNT systems. The isosurfaces of the selected frontier orbitals show that the π-electronic structures of the CNTs remain basically undamaged. This study confirms the experimental finding[37] of the key role of His and Trp when binding to the CNT surface. Our calculations predict that the noncovalent modification of SWCNTs by the active peptides might increase the former's electron transfer capabilities. These results provide a better understanding of the binding between peptides and CNTs and, therefore, have potential applications for designing biofunctionalized CNTs as biosensors and drug delivery devices.

Acknowledgment. The work described in this paper is supported by the Research Grants Council of Hong Kong SAR [project no. CityU 103907] and Centre for Applied Computing and Interactive Media (ACIM).

References

(1) Iijima, S. *Nature* **1991**, *354*, 56–58.

(2) Ajayan, P. M. *Chem. Rev.* **1999**, *99*, 1787–1799.

(3) Martin, C. R.; Kohli, P. *Nat. Rev. Drug Discovery* **2003**, *2*, 29–37.

(4) Li, J.; Ng, H. T.; Chen, H. *Methods Mol. Biol.* **2005**, *300*, 191–23.

(5) Contarino, M. R.; Sergi, M.; Harrington, A. E.; Lazareck, A.; Xu, J.; Chaiken, I. *J. Mol. Recognit.* **2006**, *19*, 363–371.

(6) Hirsch, A. *Angew. Chem., Int. Ed.* **2002**, *41*, 1853–1859.

(7) Huang, W.; Fernando, S.; Lin, Y.; Zhou, B.; Allard, L. F.; Sun, Y.-P. *Langmuir* **2003**, *19*, 7084–7088.

(8) O'Connell, M. J.; Bachilo, S. M.; Huffman, C. B.; Moore, V. C.; Strano, M. S.; Haroz, E. H.; Rialon, K. L.; Boul, P. J.; Noon, W. H.; Ma, J.; Hauge, R. H.; Weisman, R. B.; Smalley, R. E. *Science* **2002**, *297*, 593–596.

(9) Dalton, A. B.; Blau, W. J.; Chambers, G.; Coleman, J. N.; Henderson, K.; Lefrant, S.; McCarthy, B.; Stephan, C.; Byrne, H. J. *Synth. Met.* **2001**, *121*, 1217–1218.

(10) Zheng, M.; Jagota, A.; Semke, E. D.; Diner, B. A.; Mclean, R. S.; Lustig, S. R.; Richardson, R. E.; Tassi, N. G. *Nat. Mater.* **2003**, *2*, 338–342.

(11) Zheng, M.; Jagota, A.; Strano, M. S.; Santos, A. P.; Barone, P.; Chou, S. G.; Diner, B. A.; Dresselhaus, M. S.; Mclean, R. S.; Onoa, G. B.; Samsonidze, G. G.; Semke, E. D.; Usrey, M.; Walls, D. J. *Science* **2003**, *302*, 1545–548.

(12) Numata, M.; Asai, M.; Kaneko, K.; Bae, A.-H.; Hasegawa, T.; Sakurai, K.; Shinkai, S. *J. Am. Chem. Soc.* **2005**, *127*, 5875–5884.

(13) Dieckmann, G. R.; Dalton, A. B.; Johnson, P. A.; Razal, J.; Chen, J.; Giordano, G. M.; Muñoz, E.; Musselman, I. H.; Baughman, R. H.; Draper, R. K. *J. Am. Chem. Soc.* **2003**, *125*, 1770–1777.

(14) Zorbas, V.; Ortiz-Acevedo, A.; Dalton, A. B.; Yoshida, M. M.; Dieckmann, G. R.; Draper, R. K.; Baughman, R. H.; Jose-Yacaman, M.; Musselman, I. H. *J. Am. Chem. Soc.* **2004**, *126*, 7222–7227.

(15) Ortiz-Acevedo, A.; Xie, H.; Zorbas, V.; Sampson, W. M.; Dalton, A. B.; Baughman, R. H.; Draper, R. K.; Musselman, I. H.; Dieckmann, G. R. *J. Am. Chem. Soc.* **2005**, *127*, 9512–9517.

(16) Karajanagi, S. S.; Yang, H.; Asuri, P.; Sellitto, E.; Dordick, J. S.; Kane, R. S. *Langmuir* **2006**, *22*, 1392–1395.

(17) Pender, M. J.; Sowards, L. A.; Hartgerink, J. D.; Stone, M. O.; Naik, R. R. *Nano Lett.* **2006**, *6*, 40–44.

(18) Su, Z.; Leung, T.; Honek, J. F. *J. Phys. Chem. B* **2006**, *110*, 23623–23627.

(19) Burley, S. K.; Petsko, G. A. *Adv. Protein Chem.* **1988**, *39*, 125–189.

(20) Hatfield, M. P. D.; Palermo, N. Y.; Csontos, J.; Murphy, R. F.; Lovas, S. *J. Phys. Chem. B* **2008**, *112*, 3503–3508, and reference therein.

(21) Borics, A.; Murphy, R.; Lovas, S. *Biopolymers (Biospectroscopy)* **2003**, *72*, 21–24.

(22) Tsuzuki, S.; Honda, K.; Uchimaru, T.; Mikami, M.; Tanabe, K. *J. Am. Chem. Soc.* **2002**, *124*, 104–112.

(23) Morita, S.; Fujii, A.; Mikami, N.; Tsuzuki, S. *J. Phys. Chem. A* **2006**, *110*, 10583–10590.

(24) Seifert, G.; Porezag, D.; Frauenheim, Th. *Int. J. Quantum Chem.* **1996**, *58*, 185–192.

(25) Elstner, M.; Porezag, D.; Jungnickel, G.; Elsner, J.; Haugk, M.; Frauenheim, T.; Suhai, S.; Seifert, G. *Phys. Rev. B: Condens. Matter* **1998**, *58*, 7260–7268.

(26) Elstner, M.; Hobza, P.; Frauenheim, T.; Suhai, S.; Kaxiras, E. *J. Chem. Phys.* **2001**, *114*, 5149–5155.

(27) Elstner, M.; Frauenheim, T.; Suhai, S. *J. Mol. Struct.: THEOCHEM.* **2003**, *632*, 29–41.

(28) Ordejón, P.; Artacho, E.; Soler, J. M. *Phys. Rev. B: Condens. Matter* **1996**, *53*, 10441–10444.

(29) Sánchez-Portal, D.; Artacho, E.; Soler, J. M. *Int. J. Quantum Chem.* **1997**, *65*, 453–461.

(30) Ceperley, D. M.; Alder, B. J. *Phys. Rev. Lett.* **1980**, *45*, 566–569.

(31) Troullier, N.; Martins, J. L. *Phys. Rev. B: Condens. Matter* **1991**, *43*, 1993–2006.

(32) Fan, W. J.; Zhang, R. Q. *Sci. China, Ser. B* **2008**, *51*, 1203–1210.

(33) Tournus, F.; Latil, S.; Heggie, M. I.; Charlier, J.-C. *Phys. Rev. B: Condens. Matter* **2005**, *72*, 075431.

(34) Tournus, F.; Charlier, J. C. *Phys. Rev. B: Condens. Matter* **2005**, *71*, 165421.

(35) Enyashin, A. N.; Gemming, S.; Seifert, G. *Nanotechnology* **2007**, *18*, 245702.

(36) Lin, C. S.; Zhang, R. Q.; Niehaus, T. A.; Frauenheim, T. *J. Phys. Chem. C* **2007**, *111*, 4069–4073.

(37) Wang, S.; Humphreys, E. S.; Chung, S. Y.; Delduco, D. F.; Lustig, S. R.; Wang, H.; Parker, K. N.; Rizzo, N. W.; Subramoney, S.; Chiang, Y. M.; Jagota, A. *Nat. Mater.* **2003**, *2*, 196–200.

(38) Cheng, Y.; Liu, G. R.; Li, Z. R.; Lu, C. *Physica A* **2006**, *367*, 293–304.

(39) Tomásio, S. D.; Walsh, T. R. *Mol. Phys.* **2007**, *105*, 221–229.

CT9002493